NIPPON STEEL TECHNICAL REPORT No. 66 JULY 1995

UDC624.014.25:711.4

Development of Elevated Steel Structures in Cities

Yasushi Fujita*1
Tetsurou Nose*1
Shunsuke Machino*1
Susumu Nakazawa*1
Hiroyuki Asaoka*1
Hiromichi Yasunami*2
Tadahiko Mori*2
Toshio Sasaki*1

Abstract:

Using steel structures featuring excellent deformation performance and lightness is expected to improve the earthquake-resistance of elevated structures in urban areas. Introduced here are trial designs of (1) steel bridge piers made of extra-thick-walled steel pipe as substitutes for conventional concrete bridge piers and thin-walled multiple-stiffened steel box piers and, (2) labor-saving steel decks as substitutes for conventional steel decks supported by many cross ribs and in need of improved fatigue strength and fabricability. For the former elevated structure, the revision of applicable standards for the adoption of extra-thick-walled steel pipes is proposed based on the buckling strength verification of the steel pipes by compression test. To confirm the ease of construction, horizontal joints were welded between extra-thick-walled steel pipes to simulate on-site welding conditions by using a Nippon Steel-developed automatic welding machine. The welded steel pipes were bend tested to ascertain the soundness of the horizontal weld joints. The latter (improved steel deck) was compared with the conventional steel deck in terms of not only steel weight but also the number of pieces and length of all welds. The advantage of using the improved steel deck for reducing construction costs was verified.

1. Introduction

Steel viaducts are usually constructed because of poor ground conditions, long span, or complicated road alignment. Damage of viaducts in the Great Hanshin Earthquake of January 1995 reconfirmeded the aseismic superiority of steel structures that are lighter and have excellent deformation capacity compared with concrete structures. When a steel structure is damaged to some degree, its cracks can be easily repaired by welding, and it can be easily reinforced by installing stiffeners. Concrete structures are not so easy to repair. The recyclability of steel is well recognized compared with concrete that creates large amounts of industrial waste when damaged or when failed concrete structures are demolished. This article studies economical urban elevated steel structures with the aim of encouraging a greater adoption of steel structures with excellent seismic performance for main roads in

*1 Engineering Divisions Group *2 Technical Development Bureau

cities.

Present steel bridge pier structures do not fully demonstrate their potential deformation capacity. Thin-walled multiple-stiffened steel piers, a design to minimize steel weight, undergo local buckling before their ultimate strength is called into play, and cannot deliver post-yield strength as required in earthquakes. For the fabrication of steel girders, minimization of the total fabrication cost or construction cost by reducing the fabrication labor component is being studied as an approach different from the minimum steel weight criteria. Using piers made of steel pipe, measuring 50 mm or more in wall thickness, in place of thin-walled multiple-stiffened steel box piers is expected to achieve both the improvement in deformation capacity and the reduction in total construction cost. Extra-thick-walled steel pipes can be built with such careful control in the plate stage that they can be bent to a radius smaller than 15 times the wall thickness as described in the Specifications for Highway Bridges (SHB) of the Japan Road Association[1] without adversely affecting strength and other properties. The diameter of steel pipes for bridge piers in urban areas can be reduced by increasing the wall thickness. From a space-saving point of view, extra-thick-walled steel pipes are also advantageous in cities where bridge piers are often erected on the median strips of existing roads. This article studies the technical problems associated with the adoption of extra-thick-walled steel pipe piers, and verifies their feasibility and advantages.

The weight proportions of prestressed concrete (PC) girders, reinforced concrete (RC) deck steel plate girders, and steel deck plate girders are about 3:1.7:1. Given its earthquake resistance, the advantages of the steel deck plate girder are recognized anew for urban viaducts, many of which are built of multiple-level construction to make effective use of limited space and are supported by many piers. Traditionally, steel decks have been often shunned because of their high cost compared with RC decks. Further improvement in the economy of steel decks can be expected from the adoption of such steel deck structures that allow for the advanced automation of steel deck fabrication, as represented by the development of an automatic multiple-electrode welding machine and a panel reforming machine. The automation of steel deck fabrication has been hindered by the welding of cross ribs to the deck plate. This process is difficult to automate and in need of structural improvement from the standpoint of fatigue strength as well. The last part of this report will focus on stiffening the structure of the steel deck by cross ribs and study an improved steel deck structure that costs less to fabricate.

2. Proposal of Steel Bridge Piers Made of Extra-Thick-Walled Steel Pipes

2.1 Background

Today's viaduct structures in cities are increasing in complexity because they must be built in limited space. Since it is particularly difficult to acquire land for roads in cities, many roads are elevated above existing roads or constructed across rivers. Median strips, sidewalks, and other limited spaces are put to effective use in constructing bridge piers of reduced section for elevated roadways. Many T-shaped bridge piers constructed on median strips of ground level roads are reported to have been damaged in the Great Hanshin Earthquake. As an alternative to conventional thin-walled multiple-stiffened steel box columns, extra-thick-walled steel pipe columns fully capable of retaining their ultimate load carrying capacity in earthquakes and their applications were studied.

The SHB prescribes that the allowable cold bending radius of steel should be at least 15 times its thickness. Steel pipe columns, measuring 900 mm in diameter and 90 mm in wall thickness and made of JIS G 3106 Grade SM570Q steel, were used in large quantities in the Yokohama Landmark Tower, a high-rise building in Yokohama. Formed by the press bend process extra-thick-walled steel pipes are seam welded by the submerged arc welding (SAW) process. Composition adjustment in the plate stage and other technological innovations implemented to prevent the deterioration of steel properties during the pipe forming and welding steps are not described here. There are many SHB requirements to be reviewed considering the progress of steel technology in recent years, including the provisions about the maximum steel plate thickness of 50 mm and the allowable bending radius as noted above. This article introduces the basic evaluation of strength properties of extra-thick-walled steel pipe columns and the trial design of extra-thick-walled steel pipe columns as applied to actual urban steel bridge piers, and reports the experimentally verified soundness of shop welds and automatic on-site welds that allows steel bridge piers to be fabricated from extra-thick-walled steel pipes.

2.2 Buckling strength of cold-formed thick-walled steel pipes

Thick-walled steel pipes cold formed by the press bending process were compression tested to determine their buckling strength. The buckling design method of thick-walled steel pipes was studied by comparing the compression test results with the buckling strength requirements specified in various design standards.

2.2.1 Compression test method and results

Rolled steel plates (JIS G 3106 Grade SM570) were press bent to from thick-walled steel pipes and compression tested. Each pipe measured 400 mm in external diameter and 10 mm in wall thickness. Two short-column specimens (S-1 and S-2) were used to obtain stress-strain curves in the compression region of the pipe steel, and three long-column specimens of different lengths (L-1 to L-3) were used to evaluate the buckling of the pipe steel. The S-2 specimen was annealed to remove the stress induced during the pipe forming step. The structural performance and parameters of the compression test specimens are given in **Table 1**.

The compression test was conducted at Nippon Steel's Sagamihara Research & Engineering Center using a 1,000-ton structure testing machine. The loading section was equipped with spherical seats to support the specimen by pins at both ends. Loading was uniformally increased and switched from the load control mode in the initial stage to the displacement control mode in the later stage when nonlinearity appeared. markedly

Table 1 shows the maximum strength and observed buckling mode of each specimen. The two short-column specimens each underwent circumferentially uniform convex deformation close to one pipe end, gradually became more deformated, and eventually exhibited their maximum strength. Two of the three long-column specimens, or L-1 and L-2, declined in buckling strength as soon as they buckled in the middle. With the specimen L-3, slight pipe-end convex buckling occurred first, but its final buckling strength depended on the buckling of the midlength.

Fig. 1 shows the stress-axial strain curves of the specimens as obtained from load and displacement measurements. The stress-relieved specimen S-2 remained linear until buckling, while

Table 1 Structural performance and compression test results of thick-walled steel pipe specimens

Specimen		Value calculated from nominal yield stress			Compression test results	
Name	L (mm)	L/r	λ	σ_{cr} (SHB) (N/mm²)	σ_{max} (N/mm²)	Ultimate buckling mode
S-1	1,200	5.8	0.087	450	670	Pipe end buckling
S-2	1,200	5.8	0.087	450	621	Pipe end buckling
L-1	6,000	40.6	0.606	340	569	Overall buckling (midlength)
L-2	4,000	26.1	0.389	393	641	Overall buckling (midlength)
L-3	2,000	11.6	0.173	446	663	Overall buckling (midlength)

Notes: 1) Steel type: JIS G 3106 Grade SM570 with nominal yield point of 450 N/mm²

2) Section parameters: Radius-thickness (R/t) ratio = 20.0
Radius-thickness ratio parameter (R_t) = 0.071

$$R_t = \frac{R_c}{t} \cdot \frac{\sigma_y}{E} \sqrt{3(1-\nu^2)}$$

3) Column parameters
Slenderness ratio: $L/r = L/\sqrt{I/A}$

Slenderness ratio parameter: $\lambda = \frac{1}{\pi}\sqrt{\frac{\sigma_y}{E}}\frac{kl}{r}$

(Effective buckling length was put at kl = L−400 to suit test conditions.)

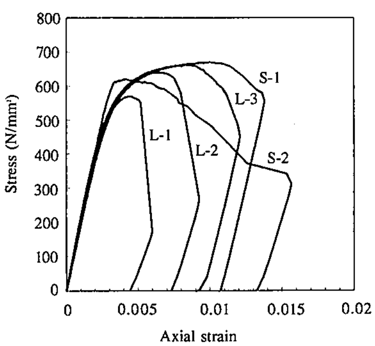

Fig. 1 Stress-axial strain curves

the non-stress-relieved specimens S-1 and L-1 to L-3 increase in nonlinearity as the compressive load increased. Stress-relief annealing not only removes residual stress, but also restores the stress-strain relationship to the condition before being formed into pipes. Stress-relieved steel pipe members exhibit linear elastic behavior until they buckle. Even below their buckling strength, non-stress-relieved steel pipe members exhibit nonlinear response mainly under the influence of residual stresses.

2.2.2 Specification of buckling strength of steel pipe members in design standards

In Japan, the buckling design of steel pipes is performed by using the buckling strength curve set forth in the SHB. When thick-walled pipes are designed according to the buckling strength curve, their measured buckling strength is much higher than the buckling strength prescribed in the SHB, as evident from comparison of the calculated and measured values of buckling strength shown in **Table 1**. The reason is that the SHB applies one specified strength as yield strength for evaluating the buckling strength of different steels of the same grade, and cannot adequately evaluate the actual yield stress of these steels.

Foreign specifications prescribe the design of steel pipe members according to the buckling strength curves that take the yield strength of steel pipe members into account. For example, the ECCS (Eurocode 3)[2)] specifies that of five buckling strength curves, an appropriate one should be selected and used to suit the cross-sectional shape and manufacturing process of specific members. It is also prescribed to use Curve A for steel pipe members that are hot worked or heat treated to remove residual stresses and to use Curve C for cold-formed steel pipe members. ISO/TC 167 (draft)[3)] has the same buckling strength curves as the ECCS. The draft also states that when a steel pipe member is short-column buckling tested, the yield point (strength) obtained in the test should be applied to the strength calculation formula (the same as Curve C of the ECCS) to set the buckling strength of the steel pipe member. A feature of this technique is that it can obtain rational design values based on yield strength because it checks the necessary buckling strength based on the actual buckling strength of the material to be used. The technique is limited to the application to thick-walled and large-diameter steel pipes that are difficult to test in their full-size section.

2.2.3 Comparison of specified and measured values of buckling strength

Figs. 2(a) to **2**(c) show the buckling strength curves SHB, ECCS-a, and ECCS-b in combination with the compression test results discussed in Section 2.2.1. The compression test results are given as the maximum buckling strength σ_{max} made dimensionless by the yield point σ_y of steel. The yield point σ_y is the specified nominal yield point (450 N/mm²) of steel in **Fig. 2**(a); the lower yield point (631 N/mm²) of plates before being formed into pipes in **Fig. 2**(b); and the 0.2% offset yield strength (629 N/mm²) of specimens removed from pipes. The 0.2% offset yield strength (619 N/mm²) is calculated from the short-column compression test results of the specimen S-1 as described in ISO/TC 167, and is used as the yield point σ_y in **Fig. 2**(d). The stress-strain curves shown in **Figs. 3**(1) and **3**(2) are the whole and partial enlargement of the material tensile test results used in **Figs. 2**(b) and **2**(c) and the compression test results of the short-

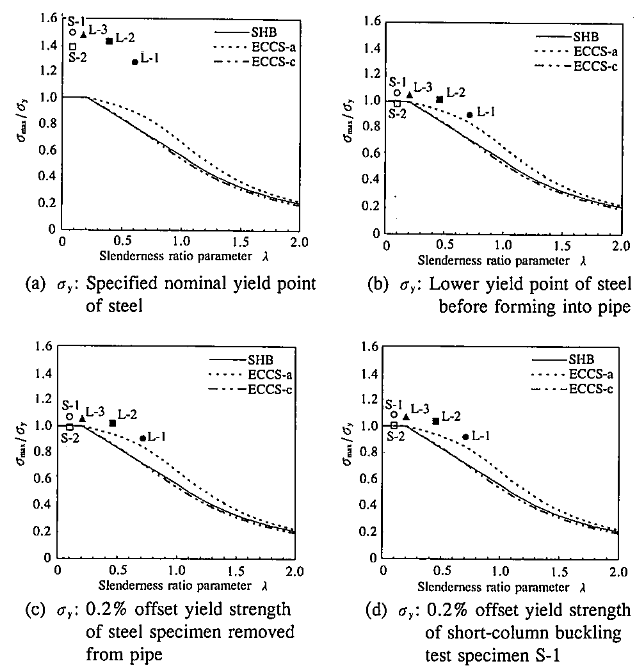

(a) σ_y: Specified nominal yield point of steel

(b) σ_y: Lower yield point of steel before forming into pipe

(c) σ_y: 0.2% offset yield strength of steel specimen removed from pipe

(d) σ_y: 0.2% offset yield strength of short-column buckling test specimen S-1

Fig. 2 Buckling strength curves

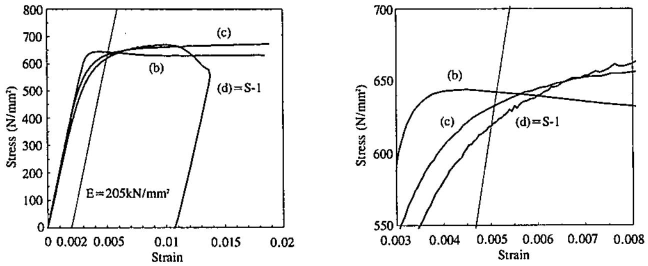

(a) Whole (b) Partial enlargement

Fig. 3 Stress-axial strain curves

column specimen S-1 used in **Fig. 2**(d) (and discussed in Section 2.2.1). The 0.2% offset yield strength curves are also shown. These results reveal the following.

The test results (a) made dimensionless by the nominal yield point of steel each greatly surpass the buckling strength curves. This is mainly because the measured yield point of the test steel is significantly higher than the specified nominal yield point, meaning that the yield strength of thick-walled steel pipes is not properly evaluated in the SHB. Similar test results are given in References 4) and 5).

In **Figs. 2**(b) and **2**(c) where the tension test results are shown, the differences between the measured and specified values are somewhat eliminated, and the measured values are much closer to the specified values. In this case, the differences between the tension and compression properties of the materials and the problem of residual stress still remain. Since application of the material tensile test results of actual steels provides evaluation on the safe side regarding the respective specifications, however, it is estimated from the test results that the ECCS-a curve can be satisfactorily used for the design of cold-formed thick-walled steel pipes. **Figs. 2**(b) and **2**(c) differ in the stress-strain relationship of the steel, depending on whether or not there is the effect of cold working. Since the test steels have almost the same yield point, they are equally evaluated in terms of buckling strength. The differences between **Figs. 2**(b) and **2**(c) appear for steels with a tensile strength of 50 kgf/mm² or less..

As discussed above, **Fig. 2**(d) uses the yield point obtained from the same short-column specimens as the buckling test specimens and reflects the compression properties of the material with allowance made for the residual stress. Similar to **Figs. 2**(b) and **2**(c), **Fig. 2**(d) indicates test results that are much closer to the ECCS-a curve. This means that an actual structural steel exhibits a value on the safe side with respect to the ECCS-a curve. Application of the short-column compression test results to the ECCS-a curve is thought to enable the rational design for thick-walled steel pipes that more accurately reflects the pipe's yield strength. For use in actual design, however, it is necessary to accumulate more data.

When the stress-relieved specimen S-2 and the non-stress-relieved specimen S-1 are compared in **Figs. 2**(a) to **2**(d), S-2 always exhibits smaller values. This is because the maximum buckling strength σ_{max} of S-2 obtained from the test results are smaller than that of S-1. Although it cannot be definitely concluded from this finding alone, it is believed that stress relieving techniques are not always effective in improving the buckling strength of steel pipes.

Based on the above-mentioned test results, the following buckling design method is proposed for thick-walled steel pipes. First, the designer selects the type of mechanical test to be conducted. Next, she/he determines from the test results the yield point σ_y to be used for evaluating the buckling strength of the pipe steel, and performs the buckling design of the steel pipe by applying the ECCS-a curve. The designer thus can more rationally design the steel pipe member by making effective use of the properties of the pipe steel and the section of the steel pipe, as compared with the present design method based on the specified nominal yield point for pipe steel and the buckling strength curve of the SHB. It is also important to study and determine whether or not stress relieving techniques are required for specific structures to be designed. It is considered especially necessary to develop design formulas that provide the correlation between the load and displacement of non-stress-relieved steel pipe members. The test cost and other factors are taken into account when determining the above-mentioned design policy.

2.2.4 Summary

When cold-formed steel pipes manufactured on an actual line were compression tested, the following findings were obtained about buckling strength evaluation and buckling design methods for steel pipe members:

(1) The maximum buckling strength obtained in the compression test is greater than any specified buckling strength, as long as the nominal yield stress is used. That is, the SHB underestimates the buckling strength of thick-walled steel pipes even when cold formed.

(2) Rational design of thick-walled steel pipes by making good use of their mechanical properties calls for preliminary mechanical tests to determine their yield point. Rational designs that more accurately reflect the mechanical properties of the pipe steel to be used can be implemented when the ISO/TC 167 technique of setting the buckling strength by using the yield point obtained in the short-column buckling test is followed.

(3) Since it is possible that stress relieving techniqus may be not always effective in improving the buckling strength of steel pipes, the designer must study and determine whether or not stress relieving is necessary for specific structures. Particularly, it will be necessary to develop design formulas for giving the correlation between the load and displacement of steel pipe members not to be stress relieved.

2.3 Trial design

2.3.1 Design conditions

The structure to be designed was an actual urban expressway as shown in **Fig. 4**, and the design conditions for the structure was set as follows:

(1) Use the section force of the actual design.

(2) Use the column height and section change position of the actual design.

(3) Set the section thickness at a maximum of 100 mm and the wall thickness difference due to the section change at a maximum of 15 mm.

(4) Set the effective buckling length of steel pipe columns at l = 2 h according to the SHB.

(5) Check the combination of stress due to axial force and stress due to bending moment according to Eqs. 3.3.4 and 3.3.5 in the SHB, and the combination of normal stress and shear stress according to Eq. 12.3.1 in the SHB.

$$\alpha_1 = \frac{\sigma_c}{\sigma_{ca}} + \frac{\sigma_{bc}}{\sigma_{ba}\left(1 - \frac{\sigma_c}{\sigma_{ea}}\right)} \leq 1 \qquad \text{SHB Eq. (3.3.4)}$$

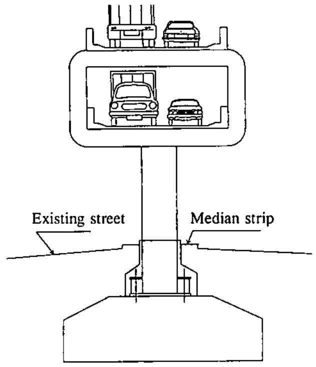

Fig. 4 Example of trial design

where σ_c = compressive stress due to axial force; σ_{bc} = compressive stress due to bending moment; and σ_{ca} = allowable compressive stress due to bending taking into consideration overall buckling.

$$\alpha_2 = \sigma_c + \frac{\sigma_{bc}}{\left(1 - \frac{\sigma_{bc}}{\sigma_{ea}}\right)} \leqq \sigma_{cal} \qquad \text{SHB Eq. (3.3.5)}$$

where σ_{ba} = upper limit value of allowable compressive stress due to bending moment; σ_{ea} = allowable Euler buckling stress; and σ_{cal} = allowable compressive stress due to bending moment taking into consideration local buckling.

$$\alpha_3 = \frac{\Sigma\sigma}{\sigma_a} + \left(\frac{\Sigma\tau}{\tau_a}\right) \leqq 1 \qquad \text{SHB Eq. (12.3.1)}$$

where σ_a = allowable normal stress; and τ_a = allowable shear stress.

2.3.2 Results of trial design

The section forces obtained by the three-dimensional analysis of the actual design are used as design section forces and summarized in **Table 2**. The results of the trial design made based on the data of **Table 2** are shown in **Table 3**, and the trial design is compared with the actual design in terms of the section of the column base in **Fig. 5**. From a space-saving point of view, the diameter of the steel pipe in the trial design is about a half as large as the diagonal length of the steel box column in the actual design. The trial design is effective in improving visibility for automobile drivers and gives a less oppressive feeling to nearby residents. The structural effect of the reduction in the cross-sectional size is studied next.

The SHB states that the allowable buckling stress of steel pipe columns of a radius not greater than 25 times the wall thickness need not be reduced for local buckling. The reduction in the allowable buckling stress compared with overall buckling due to the reduction in the section stiffness of the steel pipe columns is remarkable. The effective buckling length as shown in **Fig. 6** limits the strength of the steel. The buckling strength of steel pipes based on the compression test described in Section 2.2 should be reviewed from this standpoint.

When deflection due to live load is studied as the increase in the deflection of steel piers with the decrease in the section stiffness of steel piers, the following findings as shown in **Table 4** result. Achievable space savings depend on the pier height.

Table 2 Summary of design section forces

	P1			P2		
P_t	3,734	3,735	3,737	3,834	3,835	3,837
N_x(t)	−571.5	−580.5	−625.6	−747.5	−759.4	−822.8
M_y(tm)	−1,854.9	−2,575.2	−3,369.6	1,345.4	1,831.0	2,414.4
M_z(tm)	173.2	66.6	−46.8	−22.0	21.6	61.8
M(tm)	1,863.0	2,576.1	3,369.9	1,345.6	1,831.1	2,415.2
S_z(t)	−195.5	−197.9	−210.6	147.6	149.2	149.6
S_y(t)	29.1	29.1	29.1	−13.3	−13.3	−11.7
S (t)	197.7	200.0	212.6	148.2	149.8	150.1
T(tm)	77.8	77.8	77.8	−0.1	−0.1	−0.1

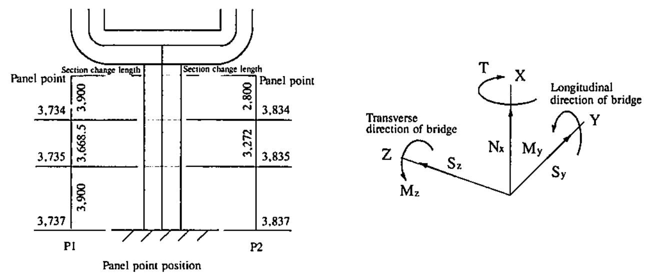

Table 3 Results of trial design

	P1			P2		
P_t	3,734	3,735	3,737	3,834	3,835	3,837
Section length (mm)	3,000.0	3,668.5	3,900.0	2,800.0	3,272.0	3,900.0
Steel grade	SM570	SM570	SM570	SM570	SM570	SM570
Pipe external diameter (mm)	1,550	1,550	1,550	1,400	1,400	1,400
Pipe wall thickness (mm)	65	80	95	60	75	90
Buckling length (mm)	24,537	24,537	24,537	23,744	23,744	23,744
Cross-sectional area (cm²)	3,032.4	3,694.5	4,342.5	2,525.8	3,122.0	3,703.9
Geometrical moment of inertia (cm⁴)	8,374,982	10,008,897	11,540,376	5,680,615	6,873,185	7,982,912
Section modulus (cm³)	108,064	129,147	148,908	81,152	98,188	114,042
Radius of gyration (cm)	52.6	52.0	51.6	47.4	46.9	46.4
R/t	11.9	9.7	8.2	11.7	9.3	7.8
1/r	46.7	47.1	47.6	50.1	50.6	51.1
$R/\alpha t$	9.9	8.1	6.8	9.7	7.8	6.5
$\sigma_c < \sigma_{ca}$	188	157	144	296	243	222
σ_{ca}	1,969	1,959	1,949	1,895	1,883	1,871
$\sigma_m < \sigma_{cal}$	1,724	1,995	2,263	1,658	1,865	2,118
σ_{cal}	2,600	2,600	2,600	2,600	2,600	2,600
$\sigma < \sigma_{ta}$	1,912	2,152	2,407	1,954	2,108	2,340
σ_{ta}	2,600	2,600	2,600	2,600	2,600	2,600
τ_s	125	103	92	112	91	76
τ_t	32	26	22	0	0	0
$\tau < \tau_a$	157	128	114	112	91	76
τ_a	1,492	1,490	1,493	1,486	1,941	1,494
$\alpha_1 < 1.0$	0.782	0.870	0.969	0.836	0.886	0.975
$\alpha_2 < \sigma_{cal}$	1,973.5	2,211.6	2,470.4	2,063.3	2,210.3	2,447.7
$\alpha_3 < 1.0$	0.747	0.835	0.932	0.757	0.815	0.903

The above discussion indicates that extra-thick-walled steel pipes can be satisfactorily applied as T-shaped pier columns for viaducts above existing streets but not for taller columns. In artificial ground composed of many pier columns, axial force is predominant, and the application of extra-thick-walled steel pipes as pier columns is advantageous from a space-saving point of view as well.

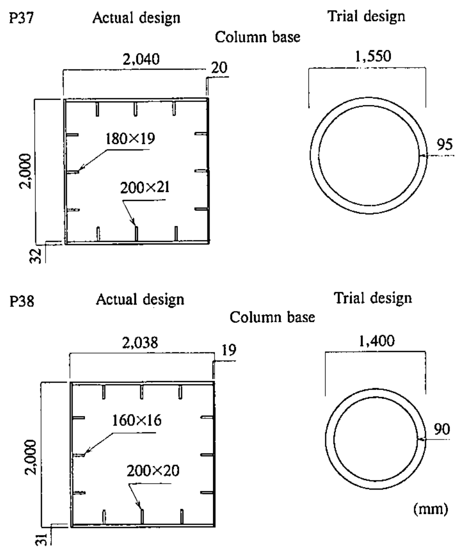

Fig. 5 Comparison of column section at base

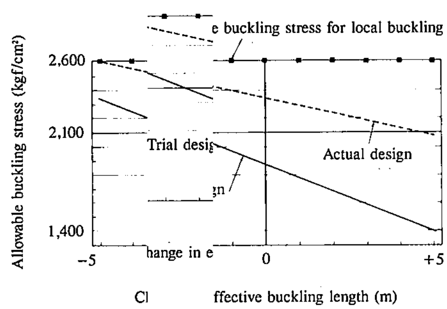

Fig. 6 Reduction in allowable buckling stress for overall buckling

Table 4 Comparison of deflection between actual design and trial design

	P37		P38	
	Actual design	Trial design	Actual design	Trial design
h (m)	11.5685		11.172	
I (m⁴)	0.16081	0.10110	0.13952	0.06972
δ (mm)	6.361	10.118	6.944	13.896

h = height of pier column
δ = deflection of column in actual design
I = average stiffness of column in actual design
δ' = deflection of column in trial design
I' = average rigidity of column in trial design
$\delta' = \frac{I}{I'}\delta$

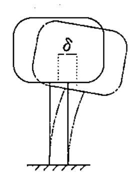

2.4 On-site welding of extra-thick-walled steel pipes

Square columns are often connected together by bolting , but steel pipe columns must be welded together on-site. Extra-thick-walled steel pipes are larger in cross-sectional area than conventional thin-walled multiple-stiffened steel box columns and thus take longer time to weld together. When conventional thin-walled multiple-stiffened steel box columns are welded during shop fabrication, they are often distorted. During on-site welding, much preparatory time must be taken to compensate for the poor groove accuracy resulting from this shop welding distortion. The edges of extra-thick-walled steel pipes can be easily prepared for on-site welding. The ease of this edge preparation is expected to improve the groove accuracy and hence the overall welding efficiency. Nippon Steel has developed and applied an automatic welding machine, designated UNI-OSCON VH, for on-site welding of steel box columns. To ascertain whether UNI-OSCON VH can be also applied to on-site welding of pier columns of greater than ever wall thickness, extra-thick-walled steel pipes were experimentally welded by UNI-OSCON VH, and the resultant weld joints were inspected for soundness.

The steel pipes used in the experiment measured 600 mm in diameter and 50 mm in wall thickness, and were made of JIS G 3106 Grade SM570Q steel. They were formed by the press bending process and seam welded by the submerged arc welding process. They were produced in two types, depending on whether or not they were annealed, in order to verify the need for annealing.

To simulate horizontal weld joints between steel pipe columns at a site, two 4.5-m long steel pipes were vertically erected one on top of the other and were welded by the automatic welding machine UNI-OSCON VH,as shown in **Photo 1**. The groove was shaped to facilitate site erection as shown in **Fig. 7**. The number of welding passes ranged from 39 to 41, and the total arc time (excluding the auxiliary work time) was 223.1 min. The steel pipes were welded under the same conditions, irrespective of whether or not they were annealed. Construction projects in urban areas generally call for shorter on-site welding time to minimize traffic control. The experiment confirmed the prospect of performing welding operations during nighttime alone.

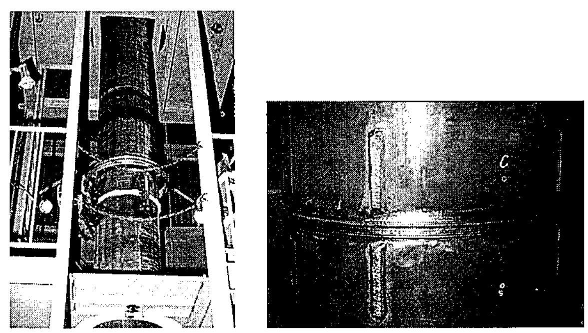

(a) (b)

Photo 1 Automatic welding of steel pipe columns

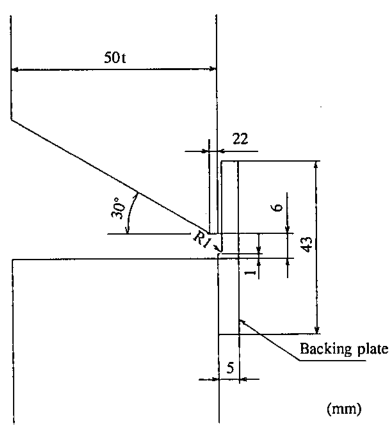

Fig. 7 Groove shape (horizontal position)

2.5 Bending experiment of extra-thin-walled steel pipes

To verify the soundness of these welds and their post-yield load carrying capacity, extra-thick-walled steel pipes were three-point bend tested on a 1,000-ton machine at Nippon Steel's Sagamihara Research & Engineering Center, as shown in **Fig 8**. The displacement-load curves of **Figs. 9** and **10** confirm that each steel pipe has a high load carrying capacity in the plastic region of the steel, be it annealed or not. The axial strain-ovality curves of **Figs. 11** and **12** show that the extra-thick-walled steel pipes flatten to an extremely small degree and have extremely stable load carrying capacity. When loaded to a central deflection of 650 to 750 mm at a span of 8 m, neither steel pipe nor the weld, developed problems, attesting to the excellent deformation capacity of extra-thick-walled steel pipes.

The flattening of steel pipes is generally approximated by the following equation. This finding about deformation performance is considered to be applicable to steel pipes of the same diameter/wall thickness ratio. The extra-thick-walled steel pipes in the trial design are expected to demonstrate a satisfactory load carrying capacity in the plastic region close to that of the trial design.

$$\Delta D/D = 0.035(D^2/\rho t)^{1.75}$$

where ΔD = amount of ovality ; D = outside diameter of steel pipe; ρ = radius of curvature; and t = wall thickness of steel pipe.

Since non-annealed pipes have a greater load carrying capacity than annealed pipes, the residual stresses developed in the pipe forming step do not necessarily have an adverse effect on the strength of steel pipes in the plastic region. This is an important result to be taken into account when considering the cost competitiveness of extra-thick-walled steel pipes.

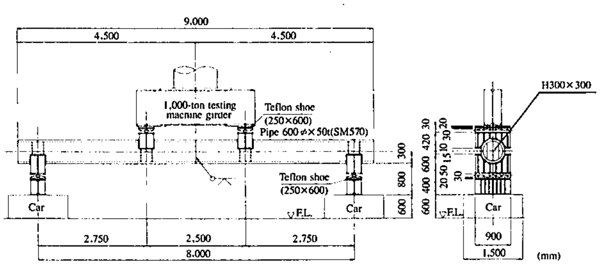

Fig. 8 Specimen setup

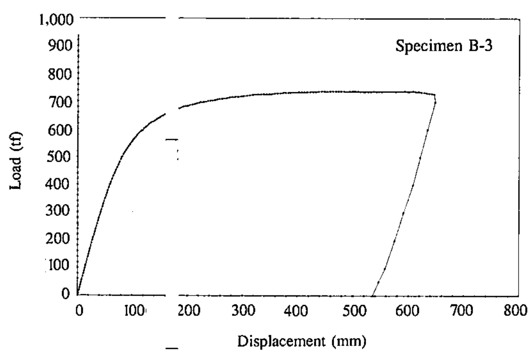

Fig. 9 Displacement-load curve (non-heat-treated specimen)

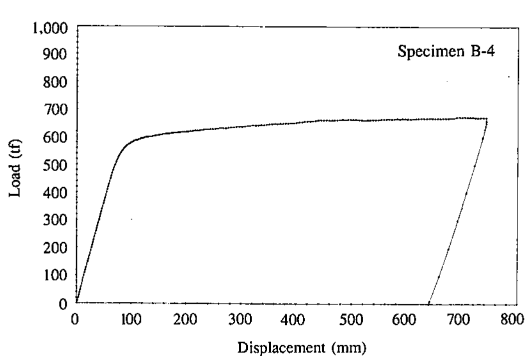

Fig. 10 Displacement-load curve (heat-treated specimen)

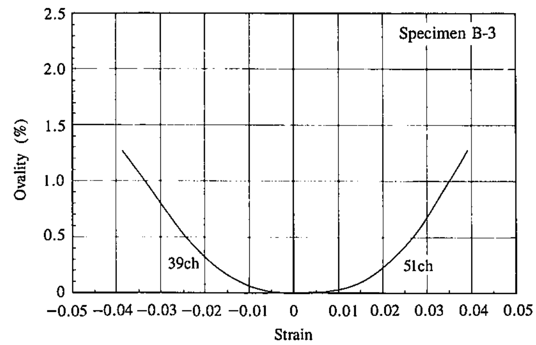

Fig. 11 Axial strain-ovality curve (non-heat-treated specimen)

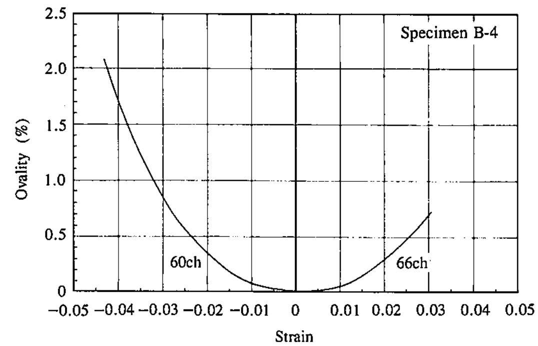

Fig. 12 Axial strain-ovality curve (heat-treated specimen)

2.6 Cost comparison

It is generally difficult to compare the cost of extra-thick-walled steel pipe columns with that of thin-walled multiple-stiffened steel box columns. Among the factors considered responsible for increasing the construction cost of extra-thick-walled steel pipe piers are: 1) increased steel weight; 2) additional cost of press bending; and 3) increased amount of on-site welding. The reduction in the number of shop fabrication hours is a cost-cutting factor. Calculations show that as the scale of bridge construction projects increases, the proportions of press bending machine setup cost and on-site automatic welding machine setup cost decrease to boost the cost competitiveness of extra-thick-walled steel pipes. Extra-thick-walled steel pipes are cost competitive where the bridge construction site is very small in area or the bridge structure must have improved in earthquake-resistant performance.

3. Proposal of Steel Deck Plate Girder Structure

3.1 Features of steel deck plate girder structures

Their economic advantage for alleviating the dead load has been recognized, but steel decks have been used only where ground conditions are poor or the span is relatively long because they are more costly to build than reinforced concrete (RC) decks. Reducing the dead load of the superstructure not only enables the economical design of the main girders, but also improves the earthquake-resistance of the bridge structure by reducing the horizontal earthquake force acting on the substructure and secondary members.

In fact, the dead weight of steel decks is only about 30 to 40% of that of RC decks, and the total dead weight of the superstructure of a steel deck plate girder bridge is about 50 to 60% of that of an RC deck girder bridge. The steel deck enhances a bridge structure's earthquakes resistance. New economical steel deck types must be developed so that more steel decks will be adopted on future bridges.

The present steel deck has a 12-mm thick deck plate reinforced with a grid arrangement of longitudinal and transverse ribs to enhance its overall rigidity, as shown in **Fig 13**. The crossing of members complicates the structure, increases the number of members and the amount of welding, and raises the number of fabrication hours and the total construction cost. The main operations required for fabricating the steel deck are as listed below.

1) Installation of longitudinal ribs at intervals of about 340 mm
2) Drilling of a huge number of holes for high-strength bolts when the members are to be bolted together on-site
3) Groove preparation and welding when the members are to be welded on-site
4) Installation of transverse ribs at intervals of about 1.5 to 3 m
5) Welding of transverse ribs in scallops where transverse ribs cross longitudinal ribs

In recent years, the efficiency of the operations 1) and 2) has been markedly improved by automation at steel bridge fabrication yards, or by drilling of high-strength bolt holes with a numerically-controlled (NC) high-speed radial drill machine and installation of longitudinal ribs with a multiple-electrode welding machine. Operation 3) has been made relatively easy to perform by the progress of NC cutting machines and field welding machines. NC robot welding machines can undertake transverse rib welding operation 4), but this operation is difficult to automate, due to the problems of inefficient intermittent welding and poor assembly accuracy.

Vehicular traffic moving on the steel deck causes fatigue damage to the deck. The main factors that are responsible for fatigue damage of the steel deck are:

1) Fatigue due to the out-of-plane deformation of the deck plate in transverse rib scallops and vertical stiffener portions
2) Fatigue due to the poor penetration of welds between the deck plate and longitudinal ribs (trough ribs) of the closed type
3) Loss of fatigue strength due to improper boxing of welds between transverse and longitudinal ribs and between transverse ribs and deck plate

Given these conditions, an improved steel deck structure is proposed that is amenable to automatic fabrication economically viable and fatigue resistant. The study results of the benefits and technical issues of the improved steel deck structure are also described.

3.2 Improved steel deck proposal

The improvements in the structural type and their objectives are summarized below.

(1) CT steel shapes are used as longitudinal ribs and placed on cross beams to eliminate the intersections of transverse ribs and cross ribs with longitudinal ribs.
(2) The thickness of the deck plate is increased to 16 mm to enhance its out-of-plane rigidity, and the longitudinal rib spacing is increased to accommodate the head of the automatic multiple-electrode welding machine.
(3) The transverse ribs are eliminated to simplify construction and reduce costs, and the longitudinal ribs are supported by the cross beams arranged at an interval of about 5 to 6 m.

The improved steel deck has CT steel shapes joined to the deck plate in the longitudinal direction alone, as shown in **Fig. 14**. Since the automatic multiple-electrode welding machine can be used extensively in the fabrication process, a sharp reduction in the number of fabrication hours is expected.

3.3 Trial design

The improved steel deck and the conventional RC deck were trial designed under the conditions of **Table 5** to compare costs. The web height of the main girders was determined from the optimum web height at which the steel weight could be minimized, and the main girders of both the steel deck and the RC deck were all made of JIS G 3106 Grade SM490Y.

The trial design results are shown in **Fig. 15**. In particular, the calculation of the construction cost took account of not only steel weight, but also the automation ratio of welding, and number of members and blocks as factors that affect the fabricability of the bridge deck.

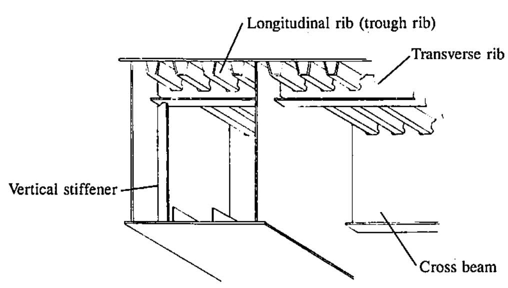

Fig. 13 Structure of conventional steel deck box girder

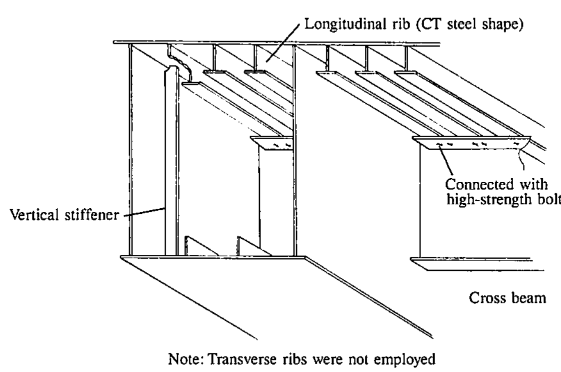

Fig. 14 Structure of improved steel deck box girder

Table 5 Design conditions

Type	Six-span continuous noncomposite box girder	Six-span continuous steel deck box girder
Load	Live load B	Live load B
Span	6×80,000m	6×80,000m
Effective width	14,000m	14,000m
Deck	RC deck (t=230 mm)	Steel deck (t=16 mm)
Pavement	Asphalt pavement (t=75 mm)	Asphalt pavement (t=80 mm)
Sectional shape	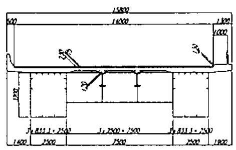	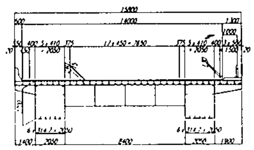

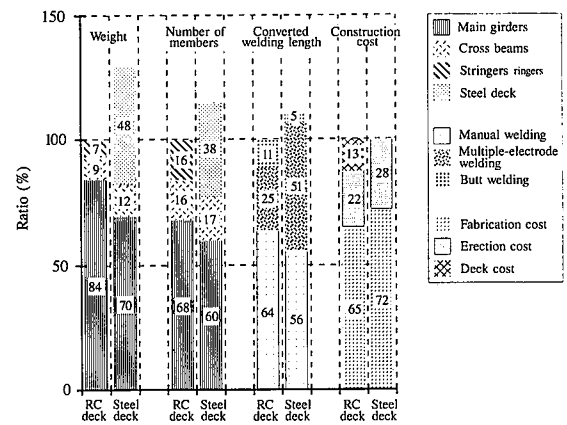

Fig. 15 Comparison of RC deck on steel plate girders and improved steel deck on steel plate girders

When compared by total weight of steel members, including main girders, cross beams and stringers but excluding the deck plate, the steel deck is about 20% lighter than the RC deck due to the reduction in the dead load. The number of members is about 10% greater for the steel deck. The converted welding length (or total length of all welds when converted to 6-mm filled welds) is greater for the steel deck, but about a half of the welds are made with efficient multiple-head welding machines. The amounts of butt welding and manual welding, which increase the fabrication hours required, are 20% smaller for the steel deck. The steel deck is slightly higher in the fabrication and erection costs, but is equal to the RC deck in the total construction cost. The results of this calculation run counter to the commonplace idea that the steel deck plate girder structure is expensive, and highlight the importance of a structure adapted to higher efficiency of fabrication.

The increase in the deck plate thickness from 12 to 16 mm increases the steel weight by about 2%, because the deck plate is part of the effective section of the main girders and because a thinner deck plate would call for longitudinal ribs to be arranged at closer spacings. Elimination of all transverse ribs was feared to sharply increase the necessary section of longitudinal ribs, but the trial design shows that the relatively small size of CT-260 × 220 × 9 × 10mm is enough for the longitudinal ribs.

3.4 Future problems

Several technical problems must be studied before the improved steel deck design can be applied to actual bridges. Main problems are summarized below.

3.4.1 Method for stiffening load concentration point at intersection of longitudinal rib and cross beam

Where a longitudinal rib and a cross beam intersect, they must be each provided with a stiffener at the support because they transmit forces to each other. This stiffening method, therefore, must be avoided to ensure rational steel deck fabrication. When the bearing stress at support is assumed to spread through the flange thickness in a 40° direction in the trial design, the developed stress is calculated to be about 1,000 kgf/cm^2 and is less than a half of the allowable compressive stress specified in the SHB. It thus suffices to stiffen the web plate to prevent its buckling. Longitudinal ribs of small web plate depth and cross beams can be significantly improved in buckling performance by slightly increasing the web plate thickness and installing a horizontal stiffer, respectively.

3.4.2 Fatigue of corner welds due to out-of-plane rotation of cross beam's top flange

When the wheel load deflects the longitudinal rib, the top flange of the cross beam rotates out of plane. When the angle of this out-of-plane rotation is large, there is the possibility that fatigue cracks may occur at the flange-to-web fillet weld. Given this possibility, it is necessary in some case to increase the rigidity of the longitudinal rib.

3.4.3 Buckling investigation of steel deck

It is necessary to confirm the overall panel buckling strength of the steel deck because the span of longitudinal ribs is increased two to three times and because longitudinal ribs of the closed type (CT section) are used. Since there are no transverse connection members between the longitudinal ribs of the steel deck, the proposed steel deck system is considered to easily suffer what is called transverse local buckling against horizontal force normal to the axis of the bridge. This problem will have to be fully studied, too.

4. Conclusions

As a result of lessons learned from the Great Hanshin Earthquake of January 1995, the current seismic standards are being reviewed to improve the safety of viaducts in cities. Any resultant rise in the construction cost of viaducts must be contained as much as possible. The labor-saving steel deck and extra-thick-walled steel pipe column systems studied in this article are based on the technological innovations achieved in recent years. They are fully cost competitive compared with conventional structural types, and designed to enhance the earthquake resistance of viaducts by reducing weight and increasing deformation capacity. Nippon Steel will work to overcome the remaining technical problems to accomplish the development of the proposed structural systems.

References

1) Japan Road Association: Specifications for Highway Bridges and Commentary, Section II - Steel Bridges. Maruzen, 1990
2) Eurocode 3: Common Unified Code of Practice for Steel Structures (draft). July 1983
3) ISO/TC 167/SC 1: Steel Structures, Materials and Design (draft). June 1991
4) Japan Society of Civil Engineers: Guidelines for Buckling Design. Gihodo, 1987, p. 88-89
5) Architectural Institute of Japan: Recommendations for the Design and Fabrication of Tubular Structures in Steel. 1990, p. 49-52